Greenland Ice Sheet Ice Slab Expansion and Thickening

Nicolas Jullien[1], Andrew Jachnik Tedstone[1], Horst Machguth[1], Nanna B. Karlsson[2], and Veit Helm[3]

[1]University of Fribourg
[2]GEUS
[3]Alfred Wegener Institute

November 23, 2022

Abstract

We use airborne accumulation radar data acquired over the Greenland Ice Sheet between 2002 and 2018 to identify changes in ice slab extent and thickness. We show that ice slabs several metres thick were already present at least as early as 2002. Between 2012 and 2018, they expanded 25,300-34,300 inland, or by 72-88%. Our results document that the extremely warm summer of 2012 produced near-surface ice layers at higher elevations, enabling ice slabs to develop in locations with only moderate melting in the following summers. With repeated flights over a transect in south-west Greenland, we show that ice slabs can thicken at the top and on their undersides. Moderate melting thickens ice slabs by top-down accretion, while large melting events can also trigger ice accretion below the slabs.

Hosted file

`essoar.10512372.1.docx` available at https://authorea.com/users/545340/articles/601994-greenland-ice-sheet-ice-slab-expansion-and-thickening

Hosted file

`jullienetal_2022_supp_submission_grl.docx` available at https://authorea.com/users/545340/articles/601994-greenland-ice-sheet-ice-slab-expansion-and-thickening

N. Jullien[1], A. J. Tedstone[1], H. Machguth[1], N. B. Karlsson[2], V. Helm[3]

[1]Department of Geosciences, University of Fribourg, Fribourg, Switzerland.

[2]Geological Survey of Denmark and Greenland, Copenhagen, Denmark.

[3]Alfred Wegener Institute, Helmholtz Centre for Polar and Marine Sciences, Bremerhaven, Germany.

Corresponding author: Nicolas Jullien (nicolas.jullien@unifr.ch)

Key Points:

- Ice slabs were already present in the early 2000s in south-west, central-west and north Greenland.
- Ice slabs expanded inland from 2002 to 2018 and get thicker by top-down accretion and by accretion on their undersides.
- Near-surface ice layers support subsequent ice slab development.

Abstract

We use airborne accumulation radar data acquired over the Greenland Ice Sheet between 2002 and 2018 to identify changes in ice slab extent and thickness. We show that ice slabs several metres thick were already present at least as early as 2002. Between 2012 and 2018, they expanded 25,300-34,300 km^2 inland, or by 72-88%. Our results document that the extremely warm summer of 2012 produced near-surface ice layers at higher elevations, enabling ice slabs to develop in locations with only moderate melting in the following summers. With repeated flights over a transect in south-west Greenland, we show that ice slabs can thicken at the top and on their undersides. Moderate melting thickens ice slabs by top-down accretion, while large melting events can also trigger ice accretion below the slabs.

Plain Language Summary

Above the equilibrium line elevation, seasonal snow is not entirely depleted by summer melting. As a result, firn - an interannual layer made of old snow and refrozen meltwater - builds up. Firn holds the potential to buffer sea level rise by trapping liquid water within its pore space. However, surface melting has increased in recent decades, making a lot of water available to percolate into the firn where it refreezes, eventually creating metres-thick ice slabs. We show that ice slabs have expanded inland and thickened from 2002 to 2018. Once formed, ice slabs continue to thicken even under moderate melt conditions. Recent increases in the ice sheet's visible runoff area match well with ice slab presence, so we conclude that ice slabs will be an important control on the future runoff area of the ice sheet.

1 Introduction

In the 1990s, the mass balance of the Greenland Ice Sheet (GrIS) was close to equilibrium, but has been negative for the last two decades (The IMBIE Team, 2020). Iceberg calving rates increased (King et al., 2020; Rignot et al., 2008; The IMBIE Team, 2020) and the surface mass balance (SMB) has been less positive as a result of increasing melt and runoff (Enderlin et al., 2014; Fettweis et al., 2017; The IMBIE Team, 2020; van den Broeke et al., 2016). Furthermore, extremely warm summers such as in 2010, 2012, 2016 and 2019 (Mikkelsen et al., 2016; Tedesco et al., 2011, 2013; Tedesco & Fettweis, 2020) triggered surface melt at high elevations with a magnitude never observed before (Hall et al., 2013; Nghiem et al., 2012) and exceptionally high volumes of runoff (Mikkelsen et al., 2016; van Angelen et al., 2014).

Recent increases in surface melting have densified the subsurface firn (Machguth et al., 2016; Mikkelsen et al., 2016; van Angelen et al., 2014). Firn is found above the equilibrium line and consists of interannual snowpack, the density of which increases by compaction through burial but also due to percolation and refreezing of surface meltwater (Braithwaite et al., 1994; Brown et al., 2011; Pfeffer & Humphrey, 1998). Firn has the potential to trap and store meltwater within its pore space, thereby buffering the GrIS contribution to sea level rise (Harper et al., 2012; Pfeffer et al., 1991).

In the percolation zone, where surface melt rates are significant, but usually do not deplete the seasonal snow completely, the fate of meltwater varies according mainly to the amount of annual snowfall. Where snowfall rates are high (~1000 +/- 400 mm w.e. per year), mostly in south-east and south Greenland, liquid water percolates to a depth where it forms perennial firn aquifers (Forster et al., 2014; Miège et al., 2016; Miller et al., 2022). Conversely, in regions where accumulation rates are lower and which have recently experienced significant melting, ice slabs several metres thick are present – mostly along the west, north and north-east of the GrIS (MacFerrin et al., 2019; Miller et al., 2022). In these regions, meltwater percolation during several successive summers fused discontinuous ice lenses into increasingly contiguous ice layers and eventually metres-thick slabs, thereby decreasing the firn's permeability (de la Peña et al., 2015; Vandecrux et al., 2019). Ice slabs form an aquitard, preventing most subsequent meltwater from reaching the relict pore space below (MacFerrin et al., 2019; Machguth et al., 2016).

Ice slabs favour the development of surface streams in the high percolation zone (Machguth et al., 2016; Mikkelsen et al., 2016; Tedstone & Machguth, 2022). The area of the ice sheet drained by surface rivers increased by 29% between 1985 and 2020, corresponding strongly with the locations of ice slabs mapped by accumulation radar (AR) (Tedstone & Machguth, 2022). This underlines that it is essential to understand firn densification and ice slab development for inclusion in ice sheet mass balance models (de la Peña et al., 2015). So far, ice slabs have only been mapped over a short time period: with AR from 2010 to 2014 (MacFerrin et al., 2019), and through a proxy approach with microwave radiometry from 2015 to 2019 (Miller et al., 2022). Here we investigate changes

in the extent and thickness of ice slabs using airborne radar observations acquired during spring-time campaigns between 2002 and 2018, and relate them to melt estimates.

2 Data and Methods

To map ice layer locations in 2002-03 we used data collected by 600-900 MHz AR (Kanagaratnam et al., 2004; Lewis, 2010) (see Fig. S5a). To map ice slabs in 2010-18, we used the 550-900 MHz AR (Carl et al., 2011; CReSIS, 2021; Rodriguez-Morales et al., 2010) (see Fig. S5b-e); the 2010-14 data are identical to those used by MacFerrin et al. (2019).

Data acquired during 2002-03 are detrended in the logarithmic domain, so they have virtually no radiometric information (J. Paden, personal communication 2020). However, the radiometric variability of the signal is large enough to enable manual ice identification (Supporting Info and Figs. 2, S1). For radar tracks acquired between 2010 and 2018, we developed a semi-automated approach based on MacFerrin et al. (2019) (more details in Supporting Info and Figures). In brief, we first picked the ice sheet surface then extracted the uppermost 100 meters. We corrected for the roll of the aircraft. To remove the impact of varying atmospheric conditions, we subtracted the average surface signal strength. We then applied a correction for depth attenuation based on MacFerrin et al. (2019).

We aim to detect changes in ice slab thickness through time. MacFerrin et al. (2019) used a normalised threshold to detect ice slabs, but we found that this approach yields strong differences between successive co-located radar tracks. Here, we utilise a range of radar signal strength as thresholds to discriminate between porous firn and ice slabs in the uppermost 20 m. First, we manually digitised ice layer features in a "reference" track acquired coincident with in-situ ground penetrating radar measurements and firn cores by MacFerrin et al. (2019) (Fig. S3). Next, we used our manually-identified ice content to determine the signal return strength given by (a) ice content versus (b) porous firn. The signal distributions of ice slabs and porous firn partially overlap (Fig. S4). Following a sensitivity analysis (Supporting Info), we chose lower and upper signal strength thresholds which correspond to the minimum and maximum likely ice content, respectively. The producer's accuracy (overall accuracy) – see Supporting Info – in detecting ice content is 53% (86%) at the lower threshold and 73% (88%) at the higher threshold (Tables S1, S2). For each radar track we also estimated the likelihood of ice slab presence between the lower and upper thresholds when ice is first detected. Thus, 100% ice likelihood corresponds to detection at the lower threshold, while 50% corresponds to detection mid-way between the lower and upper thresholds.

As a proxy for surface melting, we calculated cumulative Positive Degree Hours (cPDH) using a similar approach to degree-day modelling (Hock, 2003) – from in-situ 2 m air temperature measurements from 2009 to 2017 at the automatic weather station KAN_U (Fausto et al., 2021). We summed every positive 1-

hour average temperature (i.e. above 0°C) for each year.

3 Results

3.1 Ice slab expansion from 2002 to 2018

Ice slabs were detected in 2002-03 (Fig. 1a). Although the observations are relatively sparse (Fig. S5a), they indicate that ice slabs several meters thick were already present in SW Greenland (Fig. 2 a,c-e). Some were also identified in the CW, in the vicinity of Sermeq Kujalleq's (Jakobshavn Isbrae) high percolation zone. Ice slabs were identified in the NO but not in the NW nor the NE, although spatial coverage was limited in the latter regions.

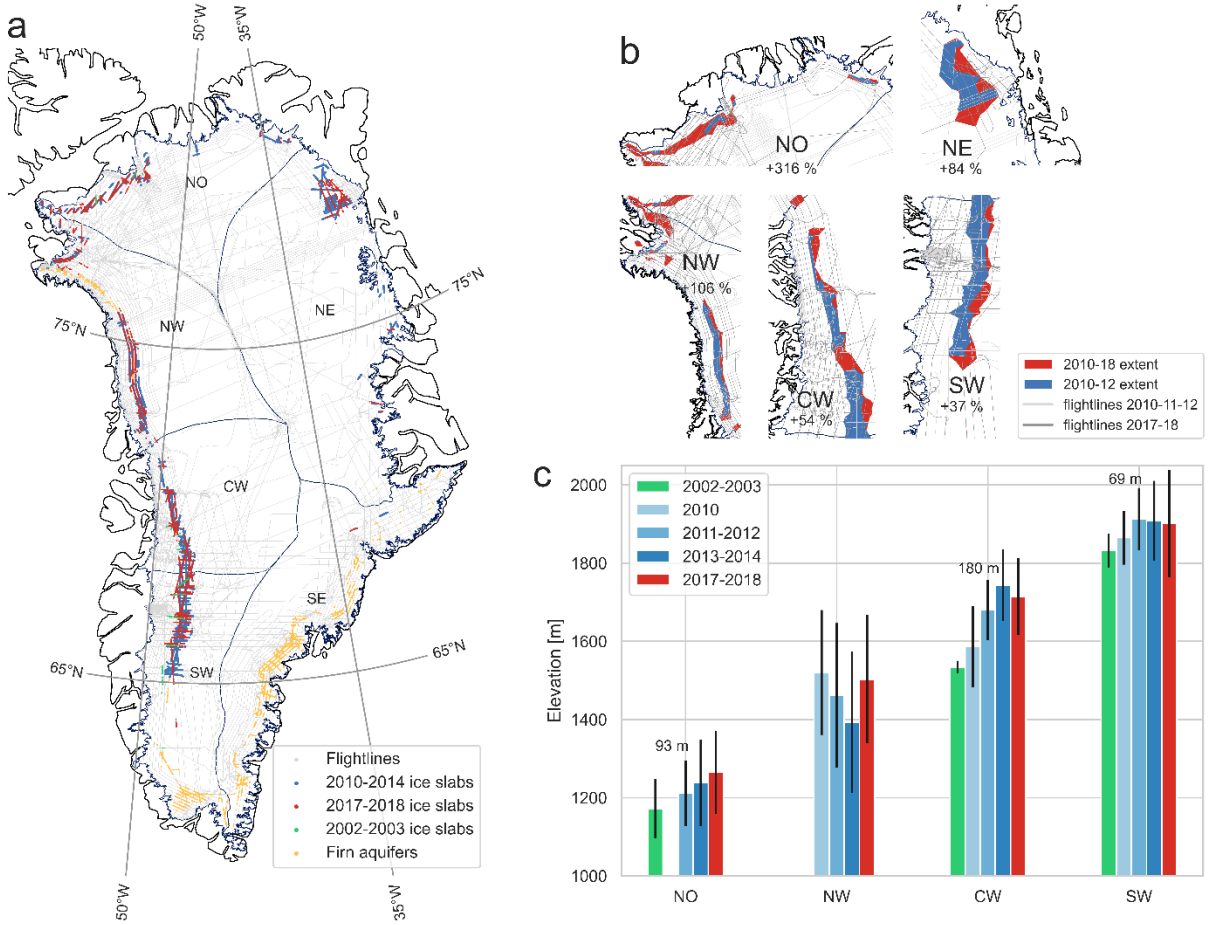

Figure 1. Ice slab presence from 2002 to 2018. (a) Ice slabs in 2002-03, 2010-14, 2017-18, and firn aquifers in 2010-2014 (Miège et al., 2016). (b) ice slabs extent in 2010-12 (blue) and 2010-18 (red). Flight lines associated with the two time periods are displayed in the background (light: 2010-12, dark: 2017-18). Percentages indicate the high-bounds of ice slabs area change by 2017-2018

with respect to 2010-12. (c) Maximum ice slabs elevation (coloured bars) +/- 1 standard deviation (black bars) in each region. Data in the NE are omitted as they are insufficient to estimate overall change. Numbers indicate the change in ice slab elevation between 2002-03 and 2017-18. Elevations are above WGS84 ellipsoid.

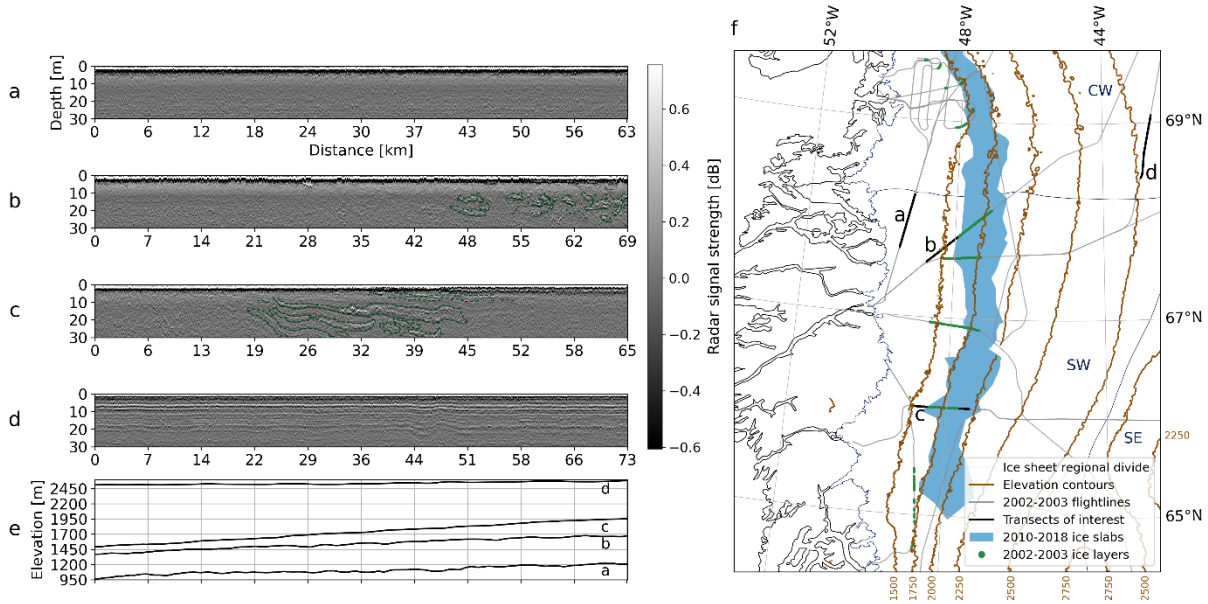

Figure 2: 30 m-deep radargrams with ice layers identification overlaid (green dashed lines) for tracks in the ablation zone (a), percolation zone (b-c), dry snow zone (d). Corresponding elevation (e) and location on the GrIS (f).

Between 2002 and 2018, ice slabs expanded to higher elevations throughout the SW, CW and NO regions (Fig. 1b,c). Except in the southern part of SW Greenland, we did not identify any entirely new ice slabs in either 2002-03 or 2017-18 compared to the 2010-14 mapping performed by MacFerrin et al., (2019) (Fig. 1a). In 2018, ice slabs extended over 60,300-73,300 km^2 (low-high bounds).

We focus on inland expansion (Fig. 1b) between 2010-12 and 2017-18. We use 2010-12 because 2011-12 has good spatial coverage in comparison to other years (Fig. S5b-e) supported by complementary coverage in 2010. Where ice slabs were already present in 2010-12, by 2017-18 they had expanded further inland. Manually outlining the extents of our slab retrievals, we estimate that ice slab area increased from 2010-12 to 2017-18 by 84% in the NE, 316% in the NO, 106% in the NW, 54% in the CW, and 37% in the SW.

We calculated the maximum ice slab elevation in each period by picking the maximum elevation in 10 km-wide boxes, then calculating the median value in each region. The maximum elevation increased in all regions except the NW

(Fig. 1c). Between 2002-03 and 2017-18 the maximum elevation increased by 93 m in the NO, 180 m in the CW, and 69 m in the SW. In the CW and SW, there is some evidence of higher maximum elevations during the intervening years between 2002-03 and 2017-18.

3.2 Ice slab thickening

The AR used to map ice slabs between 2010 and 2018 has a vertical resolution of 65cm in snow and firn (Rodriguez-Morales et al., 2014), enabling the examination of changes in ice slabs thickness. Such as MacFerrin et al., (2019), we omit ice slabs with a thickness lower than 1m and larger than 16m. We focus along six transects which had repeated radar surveys within tens to hundreds of metres during the study period (Fig. 3). Ice thickness increased between 2010 and 2018 along all the transects. While there were no major thickness changes where thick slabs were already present in 2010 (e.g. Fig. 3f from 0 to 23 km), we observed thickening of thinner ice slabs. On transect A, ice content at 11-13 km increased by 13.5 m between 2011-12 and 2017-18. On transect B, the slab at 8-15 km thickened from less than 2 m in 2010 to roughly 5 m by 2017-18.

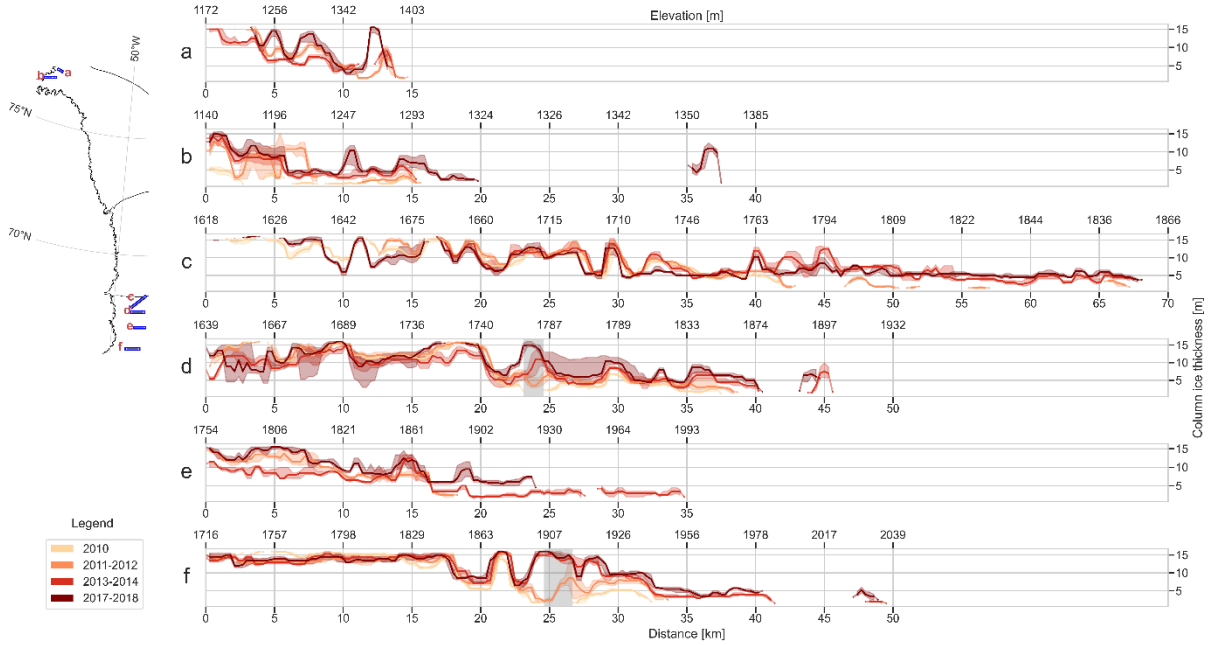

Figure 3. Ice slab thickness over time. Ice thickness in uppermost 20 m of radargrams, derived from our lower ice content detection threshold (quantile 0.79). For each transect, the data were aggregated from the start of the transect into 300 m bins, smoothed with a 900 m rolling mean. Median in bold, interquartile range denoted by shading. Equivalent elevation (m above WGS84 ellipsoid) on upper x axis.

Previously discontinuous ice slabs merged laterally over time (Fig. 3b-d,f). On transect C, a 5 to 10 m-thick ice slab developed above the 2010 upper limit (at 42 km) by 2013-14, fusing several previously thin and isolated ice layers. Consequently, the upper limit of ice slabs expanded inland by 26 km from 2010 to 2017. On transect D (Fig. 3d), the ice-free section in between 23-24.5 km (grey shading) saw initial thin ice slab generation during summer 2010. This area thickened to 15 m by 2018, filling the gap between two previously unconnected slabs and expanding the continuous ice slab by 16.5 km. Similar behaviour is apparent in transect F (Fig. 3f grey shading).

We relate ice slabs thickening with surface melting by considering a ~4 km-long transect (Fig. 4, thick dashed lines) near to the KAN_U weather station. No radar data were acquired in this area during 2002-03, but radargrams acquired nearby during 2010 and 2011 show the previous sub-surface ice content in the area (Fig. 4 a-b). We quantified the cross-sectional ice content in the upper 20 m of the sub-surface transect along almost-overlapping tracks from flights every spring from 2012 to 2018. Where the flight tracks are offset by more than a few tens of meters, retrieved ice content can vary by up to ~59 % (e.g. Fig. 4d,e, 13.8-15.6 km, where 2013 and 2014 tracks are 900-1000 m apart, see also Fig. 4i). Nonetheless, we still detected overall thickening through time (Fig. 4). From 13.8 to 17.7km, the ice content increased by 43 % between 2012 and 2018.

We used cPDH as a first-order estimate of summer melting (Fig. S6). Following the extreme melt-year of 2012 with a cPDH of 1273 ℃, ice content increased by 4,576 m^2 (19 %) from spring 2012 to spring 2013. The cPDH from summer 2013 through to 2017 was 2233 ℃ – 175% of 2012 – yet ice content increased by only 5,738 m^2 between spring 2013 and spring 2018, equivalent to 25 % more ice content formation than 2012 alone.

We observed that ice slabs can thicken by ice accretion (i) on top of existing ice content versus (ii) beneath. From 16.5 to 17.7 km (Fig. 4, in-between the right thin and right thick dashed lines), top-down ice accretion is evidenced by the thickening of the ice slab by 2.9 m while the bottom of the slab has sunk by 3 m between 2012 and 2018 (see also Fig. S7). Directly beneath KAN_U, 0.8 m of ice was added on top of the ice slab due to summer 2012 (Fig. 4c-d), while 0.6 m was added in the same way due to summer 2013 (Fig. 4d-e) even though the 2013 cPDH was only 30% of the 2012 cPDH (Fig. S6). The subsequent 2.5 m of top-down thickening between 2014 and 2018 was associated with moderate melting in 2014 and 2016 and limited melting in 2015 and 2017 (Figs. 4e-g and S6). There is further evidence of accretion on top of existing ice slabs in transects C-F (Fig. S8).

On our KAN_U transect from 13.8 to 15.6 km (Fig. 4, in-between the left thick and left thin dashed lines), ~4 m of thickening occurred predominantly beneath existing ice slabs between 2012 and 2018 (see new ice presence at 10 to 20 m depth in 2013 and 2018 compared to 2012; Figs. 4c,d,g and S7). There was ~1.5 m of median accretion after 2012 predominantly beneath the ice slab (Fig. 4c-d), while 2014-17 yielded a further ~2.5 m of median accretion split between in-

depth and top-down thickening (Fig. 4d,g). We also observed localized accretion beneath existing ice slabs in transects A, B and E (corresponding radargrams in Fig. S8). Ice slabs tend to be relatively thin where we observed ice accretion beneath them (in Fig. S8, transect A: 1-2.5 m thick, E: 5 m thick– also in Fig. 4).

Above the upper margins of the ice slab area, ice accretion takes place predominantly on top of pre-existing near-surface ice layers. At the 2012 upper ice slab boundary around 1,900 m (Fig. 4), a 6 m-thick ice slab developed by 2018 over a ~1 m thick near-surface ice layer, yielding 5.7 km inland expansion between 2012 and 2018. At higher elevations (from 25 km onwards) the near-surface ice layer was buried by subsequent accumulation.

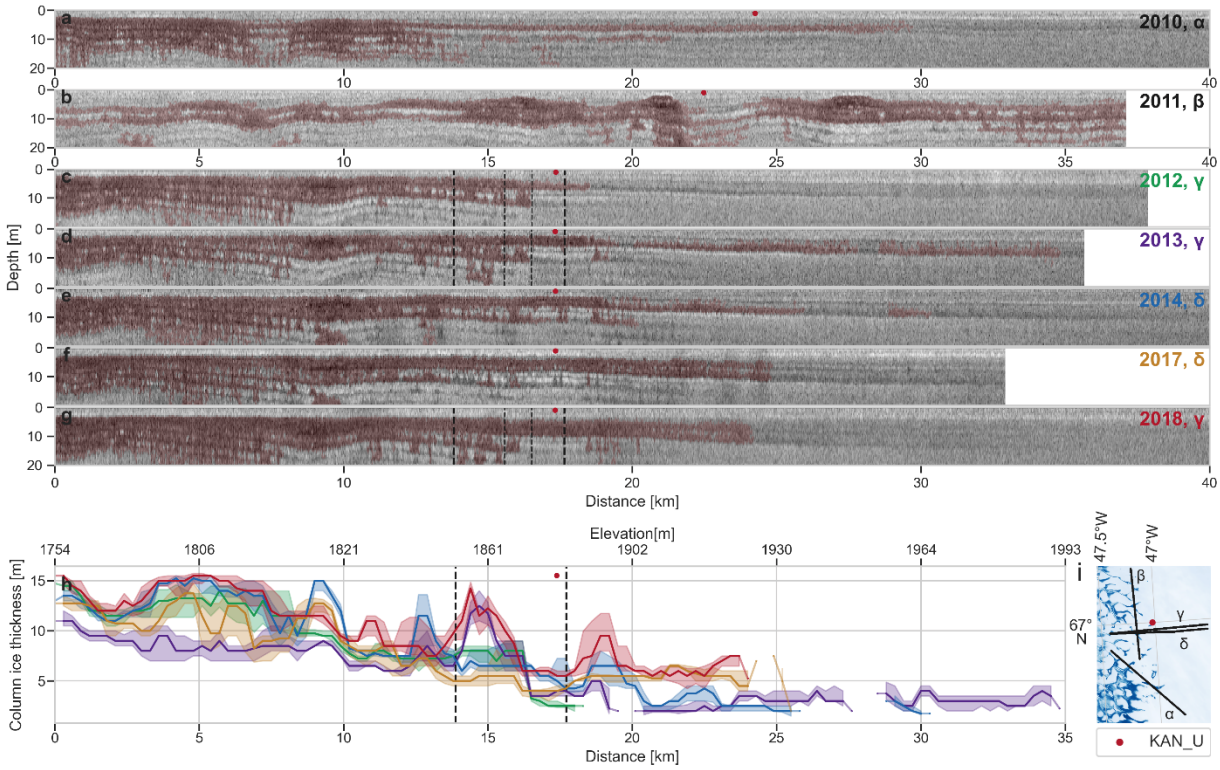

Figure 4. Ice slab thickness change through time along a transect close to KAN_U. (a-g) radar echograms in greyscale and resulting maximum likely ice content in red. (h) Total ice content in uppermost 20 m of radargrams (from 2012 onwards). Equivalent elevation (m above WGS84 ellipsoid) on upper x axis. (i) Near-infrared (band 8) Sentinel-2 image acquired on August 23rd, 2021, radargram location (black) displayed in (a-g). KAN_U station location is indicated by the red dot (c-i). In panels c, d, g and h, the thick dashed lines delineate the areas discussed in the text.

4 Discussion

4.1 Mechanisms of ice slab formation and thickening

We propose three principal mechanisms of ice slab formation and thickening. (i) Meltwater percolation and refreezing generates initial ice layers in porous firn. Then, accretion of ice by meltwater refreezing can proceed (ii) on top of, and/or (iii) beneath pre-existing ice layers.

In the data presented in Fig. 4, mechanism (i) was responsible for the initial generation of a 3 m-thick near-surface contiguous ice layer by the fusing of pre-existing discontinuous thin ice layers in porous firn from 1902 m onwards during summer 2012. Culberg et al. (2021) and de la Peña et al. (2015) similarly showed that the initiation of near-surface thin ice layers can occur within a single extremely warm summer.

Radar observations can differentiate between thickening by accretion (ii) on top of, and (iii) below existing ice content. We interpret that unexceptional but sustained melting conditions such as in 2014 or 2016 predominantly cause thickening by accretion on top of pre-existing ice slabs (Figs. 4c-g, 4). Machguth et al., (2016) also evidenced top-down ice accretion due to the 2013 and 2014 moderate melt summers comparing 2015 and 2013 cores. Hence, once ice slabs form, they continue to thicken even in moderate melt years.

The accretion that we observed below existing ice slabs (Fig. 4c-d) was primarily associated with the large cPDH during summer 2012 (Fig. S6). We propose that the abundant meltwater - that may have originated from higher elevations (Clerx et al., 2022; Machguth et al., 2016) - was able to exploit local areas of higher permeability. Previous observations show that deep percolation ($>$ 10 m) can take place in the firn without the need for wetting front advance (Humphrey et al., 2012; Machguth et al., 2016; Samimi et al., 2020). However, these processes are unlikely to occur through several meters thick ice slabs. Instead, we suggest that ice accretion beneath ice slabs takes place where large amounts of meltwater pond into slush fields or supraglacial lakes (see Fig. S9), subsequently penetrating ice slabs through fractures in the ice (Culberg et al., 2022). Indeed, crevasses are already present at high-elevations in the percolation zone of central-west Greenland (Colgan et al., 2016), providing paths for meltwater to flow vertically. Furthermore, sudden firn warming at 5 m depth at KAN_U in September 2012 is compelling evidence of abrupt meltwater penetration through a 3 m thick ice slab, which then refroze subsequently through the rest of winter (Fig. S4 and S5a in Machguth et al., (2016)). This finding is supported by ice accretion at a depth of 5 m in between existing ice slabs, revealed by firn cores acquired in 2012 and 2013 (Fig. S4c in Machguth et al., (2016)).

4.2 Changes in sub-surface firn and implications

In SW Greenland, immediately above the current ice slab area, the sub-surface firn is primed for further ice slab development. Indeed, cores from Site J (2040

m asl) acquired in 1989 and 2017 clearly show the merging of ice lenses into several ~1 m thick layers in the uppermost 12 m (Rennermalm et al., 2021), and cores acquired at Dye-2 (2,120 m asl) in 1998 and 2013 tell a similar story (Machguth et al., 2016). The increase in firn density and ice content is consistent with recent warmer surface conditions (de la Peña et al., 2015; Machguth et al., 2016).

Surface melting is projected to increase in the percolation zone (Fettweis et al., 2013; Franco et al., 2013), and extreme summer melting events such as 2010 and 2012 are expected to become more frequent (Bevis et al., 2019). Yet, radargrams indicate that further development of the near-surface ice layer generated in summer 2012 varied by elevation.

Towards the lower elevations of the thin ice layer (from ~1900m onwards) in Fig. 4 that was mostly generated due to summer 2012, additional ice accreted onto it forming ice slabs by 2017-18. Conversely, towards higher elevations where further melt between 2013 and 2017 was infrequent (Fig. S6), the near-surface layer generated in 2012 has been progressively buried to moderate depths, reducing the likelihood that it will support ice slab growth in the future. The upper limit of the summer 2012 ice layer (Fig. 4d) is located 260 m away from the location of Core 3 (Rennermalm et al., 2021). The layer probably corresponds to the numerous ice layers found in the uppermost 9 m of Core 3 in 2013. By 2019, these ice layers had been buried and could no longer be identified by radar (Fig. 4e-g), in agreement with ~3.5 m of firn replenishment identified by the redrilling of Core 3 in 2019. This is consistent with Culberg et al. (2021), who showed that the 2012 near-surface melt layer above 2600 m asl in central Greenland was initially located at 1 m deep, and was still present in 2017 but had been buried to a depth of 5 m. Thus, the ability of near-surface ice layers to support subsequent ice slab development is likely to depend on whether strong local melting occurs during several successive summers.

Considering recent sub-surface changes between 2013 and 2017, cores at KAN_U (Fig. 6a in Rennermalm et al. (2021)) show that the top of thick ice was at roughly the same depth in 2017 as 2013. We observed 0.25 m of new firn between 2013 and 2014 (Fig. 4d,e - 16.5 to 17.7 km), while the 2015 and 2016 cores also show some evidence of firn replenishment. We suggest that this replenishment subsequently melted during summer 2016 (Fig. S6) and refroze on top of the slab. Then, from 2017 to 2018, the top of ice slab deepened by 0.6 m (Fig. 4f,g), similar to Rennermalm et al. (2021) (~+0.5 m). Thus, individual years of firn replenishment which temporarily bury an ice slab can be easily erased by relatively moderate melting.

5 Conclusions

We interpreted AR data to show that ice slabs already existed in 2002-03 in SW, CW and NO Greenland, which are most likely a result of increasing surface melting from the mid-1990s onwards (van As et al., 2016). On an ice-sheet-wide basis we showed that ice slabs expanded inland from 2012 to 2018 by 25,300-

34,300 km^2, or 72-88%.

We identified two locations at which ice slabs thicken: ice accretion on top of pre-existing ice slabs, and more localised ice accretion beneath pre-existing ice slabs. We suggest that deep percolation through ice layers takes place beneath ponded surface meltwater features and exploits local fractures in otherwise near-impermeable ice slabs. Accretion below pre-existing ice slabs is therefore more likely during extreme melt seasons, while more moderate melt seasons predominantly result in top-down thickening.

Extremely warm summers such as 2012 can produce sufficient meltwater at higher elevations to generate a near-surface ice layer on the order of at least a metre thick, forming the basis for subsequent ice slab expansion via top-down ice accretion. Once formed, ice slabs continue to thicken, even under moderate melting conditions.

We suggest that future increases in melting at higher elevations will trigger further ice slab development, increasing the ice slab area non-linearly with elevation because of the non-linearity of the hypsometry of the ice sheet (Bauer, 1955). The recent expansion of the visible runoff area of the Greenland Ice Sheet is strongly linked with the extent of ice slabs (Fig. S10) (Tedstone and Machguth, 2022), so future increases in ice slab area are likely to further increase the area which contributes runoff to the oceans.

Acknowledgments

This work was funded under the European Research Council award 818994 – CASSANDRA. We acknowledge the use of data and data products from CReSIS generated with support from the University of Kansas, NASA Operation IceBridge grant NNX16AH54G, NASA grant NNX10AT68G, NSF grants ACI-1443054, OPP-1739003, and IIS-1838230, ANT-0424589, Lilly Endowment Incorporated, and the Indiana METACyt Initiative. We thank P. Bednawrek (University of Fribourg) for computational support.

Open Research

2002-2003 and 2010-2018 accumulation radar data (CReSIS, 2021) are available on the CReSIS data repository (https://data.cresis.ku.edu/data/accum/). We used the ArcticDEM digital elevation model at 100m resolution, which provides elevation above the WGS84 ellipsoid (https://www.pgc.umn.edu/data/arcticdem/). The regional divisions of the GrIS are based on the Greenland Ice Sheet drainage basins from Rignot & Mouginot (2012). Air temperatures at the automatic weather station KAN_U station can be downloaded from https://doi.org/10.22008/promice/data/aws. Sentinel 2 satellite images can be downloaded at https://scihub.copernicus.eu/dhus/#/home. The scripts used to perform the analysis for this study can be found at https://github.com/jullienn/changing_Greenland_iceslabs. Our ice slab dataset is available at https://doi.org/10.5281/zenodo.6981378.

Author contributions

NJ, AT and HM designed the study. NK contributed to interpretation of the 2002-03 radargrams. NJ developed the methodology for ice identification in 2010-18 data, with contributions from VH, HM and AT. NJ carried out data processing, data analysis and interpretation. NJ and AT wrote the manuscript based on comments from all co-authors.

References

Bauer, A. (1955). The Balance of the Greenland Ice Sheet. *Journal of Glaciology*, *2*(17), 456–462. Cambridge Core. https://doi.org/10.3189/002214355793702271Bevis, M., Harig, C., Khan, S. A., Brown, A., Simons, F. J., Willis, M., Fettweis, X., van den Broeke, M. R., Madsen, F. B., Kendrick, E., Caccamise, D. J., van Dam, T., Knudsen, P., & Nylen, T. (2019). Accelerating changes in ice mass within Greenland, and the ice sheet's sensitivity to atmospheric forcing. *Proceedings of the National Academy of Sciences*, *116*(6), 1934–1939. https://doi.org/10.1073/pnas.1806562116Braithwaite, R. J., Laternser, M., & Pfeffer, W. T. (1994). Variations of near-surface firn density in the lower accumulation area of the Greenland ice sheet, Pâkitsoq, West Greenland. *Journal of Glaciology*, *40*(136), 477–485. Cambridge Core. https://doi.org/10.3189/S002214300001234XBrown, J., Harper, J., Pfeffer, W. T., Humphrey, N., & Bradford, J. (2011). High-resolution study of layering within the percolation and soaked facies of the Greenland ice sheet. *Annals of Glaciology*, *52*(59), 35–42. https://doi.org/10.3189/172756411799096286Carl, L., Lewis, C., Gogineni, P., Rodriguez, F., Paden, J., & Li, J. (2011). *IceBridge Accumulation Radar L1B Geolocated Radar Echo Strength Profiles, 2010, 2011, 2012, 2013, 2014, 2017, 2018 [Dataset].* Boulder, Colorado USA: National Snow and Ice Data Center. Digital media. https://data.cresis.ku.edu/data/accum/.Clerx, N., Machguth, H., Tedstone, A., Jullien, N., Wever, N., Weingartner, R., & Roessler, O. (2022). *In situ measurements of meltwater flow through snow and firn in the accumulation zone of the SW Greenland Ice Sheet* [Preprint]. Ice sheets/Glacier Hydrology. https://doi.org/10.5194/egusphere-2022-71Colgan, W., Rajaram, H., Abdalati, W., McCutchan, C., Mottram, R., Moussavi, M. S., & Grigsby, S. (2016). Glacier crevasses: Observations, models, and mass balance implications: Glacier Crevasses. *Reviews of Geophysics*, *54*(1), 119–161. https://doi.org/10.1002/2015RG000504CReSIS. (2021). *Accumulation radar Data, 2002, 2003, 2010, 2011, 2012, 2013, 2014, 2017, 2018 [Dataset] Lawrence, Kansas, USA. Digital Media.* http://data.cresis.ku.edu/Culberg, R., Chu, W., & Schroeder, D. (2022). *Shallow Fracture Buffers High Elevation Runoff in Northwest Greenland* [Other]. display. https://doi.org/10.5194/egusphere-egu22-3004Culberg, R., Schroeder, D. M., & Chu, W. (2021). Extreme melt season ice layers reduce firn permeability across Greenland. *Nature Communications*, *12*(1), 2336. https://doi.org/10.1038/s41467-021-22656-5de la Peña, S., Howat, I. M., Nienow, P. W., van den Broeke, M. R., Mosley-Thompson, E., Price, S. F., Mair, D., Noël, B., & Sole, A. J. (2015). Changes in the firn structure of the western Greenland Ice Sheet caused by recent warming. *The Cryosphere*, *9*(3), 1203–1211. https://doi.org/10.5194/tc-9-

1203-2015Enderlin, E. M., Howat, I. M., Jeong, S., Noh, M.-J., van Angelen, J. H., & van den Broeke, M. R. (2014). An improved mass budget for the Greenland ice sheet. *Geophysical Research Letters*, *41*(3), 866–872. https://doi.org/10.1002/2013GL059010Fausto, R. S., van As, D., Mankoff, K. D., Vandecrux, B., Citterio, M., Ahlstrøm, A. P., Andersen, S. B., Colgan, W., Karlsson, N. B., Kjeldsen, K. K., Korsgaard, N. J., Larsen, S. H., Nielsen, S., Pedersen, A. Ø., Shields, C. L., Solgaard, A. M., & Box, J. E. (2021). *Programme for Monitoring of the Greenland Ice Sheet (PROMICE) automatic weather station data*. 27.Fettweis, X., Box, J. E., Agosta, C., Amory, C., Kittel, C., Lang, C., van As, D., Machguth, H., & Gallée, H. (2017). Reconstructions of the 1900–2015 Greenland ice sheet surface mass balance using the regional climate MAR model. *The Cryosphere*, 19.Fettweis, X., Franco, B., Tedesco, M., van Angelen, J. H., & Lenaerts, J. T. M. (2013). Estimating the Greenland ice sheet surface mass balance contribution to future sea level rise using the regional atmospheric climate model MAR. *The Cryosphere*, 21.Fettweis, X., Hofer, S., Krebs-Kanzow, U., Amory, C., Aoki, T., Berends, C. J., Born, A., Box, J. E., Delhasse, A., Fujita, K., Gierz, P., Goelzer, H., Hanna, E., Hashimoto, A., Huybrechts, P., Kapsch, M.-L., King, M. D., Kittel, C., Lang, C., … Tedesco, M. (2020). GrSMBMIP: intercomparison of the modelled 1980–2012 surface mass balance over the Greenland Ice Sheet. *The Cryosphere*, 24.Forster, R. R., Box, J. E., van den Broeke, M. R., Miège, C., Burgess, E. W., van Angelen, J. H., Lenaerts, J. T. M., Koenig, L. S., Paden, J., Lewis, C., Gogineni, S. P., Leuschen, C., & McConnell, J. R. (2014). Extensive liquid meltwater storage in firn within the Greenland ice sheet. *Nature Geoscience*, *7*(2), 95–98. https://doi.org/10.1038/ngeo2043Franco, B., Fettweis, X., & Erpicum, M. (2013). Future projections of the Greenland ice sheet energy balance driving the surface melt. *The Cryosphere*, *7*(1), 1–18. https://doi.org/10.5194/tc-7-1-2013Hall, D. K., Comiso, J. C., DiGirolamo, N. E., Shuman, C. A., Box, J. E., & Koenig, L. S. (2013). Variability in the surface temperature and melt extent of the Greenland ice sheet from MODIS: TEMPERATURE AND MELT OF GREENLAND ICE. *Geophysical Research Letters*, *40*(10), 2114–2120. https://doi.org/10.1002/grl.50240Harper, J., Humphrey, N., Pfeffer, W. T., Brown, J., & Fettweis, X. (2012). Greenland ice-sheet contribution to sea-level rise buffered by meltwater storage in firn. *Nature*, *491*(7423), 240–243. https://doi.org/10.1038/nature11566Hock, R. (2003). Temperature index melt modelling in mountain areas. *Journal of Hydrology*, *282*(1–4), 104–115. https://doi.org/10.1016/S0022-1694(03)00257-9Humphrey, N. F., Harper, J. T., & Pfeffer, W. T. (2012). Thermal tracking of meltwater retention in Greenland's accumulation area: THERMAL TRACKING OF MELTWATER RETENTION. *Journal of Geophysical Research: Earth Surface*, *117*(F1), n/a-n/a. https://doi.org/10.1029/2011JF002083Joughin, I., Smith, B. E., & Howat, I. M. (2018). A complete map of Greenland ice velocity derived from satellite data collected over 20 years. *Journal of Glaciology*, *64*(243), 1–11. https://doi.org/10.1017/jog.2017.73Kanagaratnam, P., Gogineni, S. P., Ramasami, V., & Braaten, D. (2004). A Wideband Radar for High-Resolution Mapping of Near-Surface Internal Layers in Glacial

Ice. *IEEE Transactions on Geoscience and Remote Sensing*, *42*(3), 483–490. https://doi.org/10.1109/TGRS.2004.823451Karlsson, N. B., Colgan, W. T., Binder, D., Machguth, H., Abermann, J., Hansen, K., & Pedersen, A. Ø. (2019). Ice-penetrating radar survey of the subsurface debris field at Camp Century, Greenland. *Cold Regions Science and Technology*, *165*, 102788. https://doi.org/10.1016/j.coldregions.2019.102788King, M. D., Howat, I. M., Candela, S. G., Noh, M. J., Jeong, S., Noël, B. P. Y., van den Broeke, M. R., Wouters, B., & Negrete, A. (2020). Dynamic ice loss from the Greenland Ice Sheet driven by sustained glacier retreat. *Communications Earth & Environment*, *1*(1), 1. https://doi.org/10.1038/s43247-020-0001-2Kovacs, A., Gow, A. J., & Morey, R. M. (1995). The in-situ dielectric constant of polar firn revisited. *Cold Regions Science and Technology*, *23*(3), 245–256. https://doi.org/10.1016/0165-232X(94)00016-QLewis, C. (2010). *Airborne UHF Radar for Fine Resolution Mapping of Near-Surface Accumulation Layers in Greenland and West Antarctica, (Master's thesis)* [University of Kansas]. Retrieved from KU Scholar Works data repository (http://hdl.handle.net/1808/7008)MacFerrin, M., Machguth, H., As, D. van, Charalampidis, C., Stevens, C. M., Heilig, A., Vandecrux, B., Langen, P. L., Mottram, R., Fettweis, X., Broeke, M. R. van den, Pfeffer, W. T., Moussavi, M. S., & Abdalati, W. (2019). Rapid expansion of Greenland's low-permeability ice slabs. *Nature*, *573*(7774), 403–407. https://doi.org/10.1038/s41586-019-1550-3Machguth, H., MacFerrin, M., van As, D., Box, J. E., Charalampidis, C., Colgan, W., Fausto, R. S., Meijer, H. A. J., Mosley-Thompson, E., & van de Wal, R. S. W. (2016). Greenland meltwater storage in firn limited by near-surface ice formation. *Nature Climate Change*, *6*(4), 390–393. https://doi.org/10.1038/nclimate2899Miège, C., Forster, R. R., Brucker, L., Koenig, L. S., Solomon, D. K., Paden, J. D., Box, J. E., Burgess, E. W., Miller, J. Z., McNerney, L., Brautigam, N., Fausto, R. S., & Gogineni, S. (2016). Spatial extent and temporal variability of Greenland firn aquifers detected by ground and airborne radars. *Journal of Geophysical Research: Earth Surface*, *121*(12), 2381–2398. https://doi.org/10.1002/2016JF003869Mikkelsen, A. B., Hubbard, A., MacFerrin, M., Box, J. E., Doyle, S. H., Fitzpatrick, A., Hasholt, B., Bailey, H. L., Lindbäck, K., & Pettersson, R. (2016). Extraordinary runoff from the Greenland ice sheet in 2012 amplified by hypsometry and depleted firn retention. *The Cryosphere*, *10*(3), 1147–1159. https://doi.org/10.5194/tc-10-1147-2016Miller, J. Z., Culberg, R., Long, D. G., Shuman, C. A., Schroeder, D. M., & Brodzik, M. J. (2022). An empirical algorithm to map perennial firn aquifers and ice slabs within the Greenland Ice Sheet using satellite L-band microwave radiometry. *The Cryosphere*, *16*(1), 103–125. https://doi.org/10.5194/tc-16-103-2022Nghiem, S. V., Hall, D. K., Mote, T. L., Tedesco, M., Albert, M. R., Keegan, K., Shuman, C. A., DiGirolamo, N. E., & Neumann, G. (2012). The extreme melt across the Greenland ice sheet in 2012. *Geophysical Research Letters*, *39*(20), 2012GL053611. https://doi.org/10.1029/2012GL053611Pfeffer, W. T., & Humphrey, N. F. (1998). Formation of ice layers by infiltration and refreezing of meltwater. *Annals of Glaciology*, *26*, 83–91.

https://doi.org/10.3189/1998AoG26-1-83-91Pfeffer, W. T., Meier, M. F., & Illangasekare, T. H. (1991). Retention of Greenland runoff by refreezing: Implications for projected future sea level change. *Journal of Geophysical Research*, *96*(C12), 22117. https://doi.org/10.1029/91JC02502Rennermalm, Å. K., Hock, R., Covi, F., Xiao, J., Corti, G., Kingslake, J., Leidman, S. Z., Miège, C., Macferrin, M., Machguth, H., Osterberg, E., Kameda, T., & McConnell, J. R. (2021). Shallow firn cores 1989–2019 in southwest Greenland's percolation zone reveal decreasing density and ice layer thickness after 2012. *Journal of Glaciology*, *68*(269), 431–442. https://doi.org/10.1017/jog.2021.102Rignot, E., Box, J. E., Burgess, E., & Hanna, E. (2008). Mass balance of the Greenland ice sheet from 1958 to 2007. *Geophysical Research Letters*, *35*(20), L20502. https://doi.org/10.1029/2008GL035417Rignot, E., & Mouginot, J. (2012). Ice flow in Greenland for the International Polar Year 2008-2009: ICE FLOW GREENLAND 2009. *Geophysical Research Letters*, *39*(11), n/a-n/a. https://doi.org/10.1029/2012GL051634Robin, G. D. Q. (1975). Velocity of radio waves in ice by means of a bore-hole interferometric technique. *Journal of Glaciology*, *15*(73), 151–159. Cambridge Core. https://doi.org/10.3189/S0022143000034341Rodriguez-Morales, F., Byers, K., Crowe, R., Player, K., Hale, R. D., Arnold, E. J., Smith, L., Gifford, C. M., Braaten, D., Panton, C., Gogineni, S., Leuschen, C. J., Paden, J. D., Li, J., Lewis, C. C., Panzer, B., Gomez-Garcia Alvestegui, D., & Patel, A. (2014). Advanced Multifrequency Radar Instrumentation for Polar Research. *IEEE Transactions on Geoscience and Remote Sensing*, *52*(5), 2824–2842. https://doi.org/10.1109/TGRS.2013.2266415Rodriguez-Morales, F., Gogineni, P., Leuschen, C., Allen, C., Lewis, C., Patel, A., Byers, K., Smith, L., Shi, L., Panzer, B., Blake, W., Crowe, R., & Gifford, C. (2010). Development of a multi-frequency airborne radar instrumentation package for ice sheet mapping and imaging. *2010 IEEE MTT-S International Microwave Symposium*, 157–160. https://doi.org/10.1109/MWSYM.2010.5518197Samimi, S., Marshall, S. J., & MacFerrin, M. (2020). Meltwater Penetration Through Temperate Ice Layers in the Percolation Zone at DYE-2, Greenland Ice Sheet. *Geophysical Research Letters*, *47*(15). https://doi.org/10.1029/2020GL089211Tedesco, M., & Fettweis, X. (2020). Unprecedented atmospheric conditions (1948–2019) drive the 2019 exceptional melting season over the Greenland ice sheet. *The Cryosphere*, *14*(4), 1209–1223. https://doi.org/10.5194/tc-14-1209-2020Tedesco, M., Fettweis, X., Mote, T., Wahr, J., Alexander, P., Box, J. E., & Wouters, B. (2013). Evidence and analysis of 2012 Greenland records from spaceborne observations, a regional climate model and reanalysis data. *The Cryosphere*, *7*(2), 615–630. https://doi.org/10.5194/tc-7-615-2013Tedesco, M., Fettweis, X., van den Broeke, M. R., van de Wal, R. S. W., Smeets, C. J. P. P., van de Berg, W. J., Serreze, M. C., & Box, J. E. (2011). The role of albedo and accumulation in the 2010 melting record in Greenland. *Environmental Research Letters*, *6*(1), 014005. https://doi.org/10.1088/1748-9326/6/1/014005Tedstone, A. J., & Machguth, H. (2022). Increasing surface runoff from Greenland's firn areas. *Nature Climate Change*. https://doi.org/10.1038/s41558-022-01371-zThe IMBIE Team. (2020). Mass balance of the Greenland Ice Sheet from 1992

to 2018. *Nature*, *579*(7798), 233–239. https://doi.org/10.1038/s41586-019-1855-2van Angelen, J. H., van den Broeke, M. R., Wouters, B., & Lenaerts, J. T. M. (2014). Contemporary (1960–2012) Evolution of the Climate and Surface Mass Balance of the Greenland Ice Sheet. *Surveys in Geophysics*, *35*(5), 1155–1174. https://doi.org/10.1007/s10712-013-9261-zvan As, D., Fausto, R. S., Cappelen, J., van de Wa, R. S. W. l, Braithwaite, R. J., Machguth, H., & PROMICE project team, *. (2016). Placing Greenland ice sheet ablation measurements in a multi-decadal context. *GEUS Bulletin*, *35*, 71–74. https://doi.org/10.34194/geusb.v35.4942van den Broeke, M. R., Enderlin, E. M., Howat, I. M., Kuipers Munneke, P., Noël, B. P. Y., van de Berg, W. J., van Meijgaard, E., & Wouters, B. (2016). On the recent contribution of the Greenland ice sheet to sea level change. *The Cryosphere*, *10*(5), 1933–1946. https://doi.org/10.5194/tc-10-1933-2016Vandecrux, B., MacFerrin, M., Machguth, H., Colgan, W. T., van As, D., Heilig, A., Stevens, C. M., Charalampidis, C., Fausto, R. S., Morris, E. M., Mosley-Thompson, E., Koenig, L., Montgomery, L. N., Miège, C., Simonsen, S. B., Ingeman-Nielsen, T., & Box, J. E. (2019). Firn data compilation reveals widespread decrease of firn air content in western Greenland. *The Cryosphere*, *13*(3), 845–859. https://doi.org/10.5194/tc-13-845-2019